Passive Cooling in Aerogel-Based Insulation Systems for Liquid Hydrogen Upper Stage Launch Vehicle Tanks

A.M. Swanger[1] and M.A. Guerrero Nacif[1]

[1]NASA Kennedy Space Center, Cryogenics Test Laboratory, KSC, FL 32899 USA

**Corresponding Author:* adam.m.swanger@nasa.gov

Abstract

Spray-On Foam Insulation (SOFI) is typically used to protect the windward-facing side of flight tanks for space launch vehicle liquid hydrogen (LH_2) stages. SOFI is an excellent insulator in ambient pressure environments, however, its performance pales in comparison to reflective-type systems such as Multi-Layer Insulation in the thermal radiation dominated vacuum environment of space. If a windward insulation system employing radiation shields could be devised to replace or supplement SOFI, the on-orbit heat load could be drastically reduced, and the residual propellants could then be used to facilitate secondary missions. Such insulation systems, utilizing aerogel blanket insulation, have been explored by the Cryogenics Test Laboratory at NASA Kennedy Space Center. Owing to its nano-porous structure, aerogel is an excellent adsorbent as well as an insulator at cryogenic temperatures and will readily uptake condensable background gasses such as air when protecting a surface near LH_2 temperatures. When an adsorbed blanket is rapidly exposed to a vacuum, such as during the ascent of a rocket, it will release the background gas, producing a passive cooling effect that could potentially reduce or eliminate the heat load on the propellant tank for a time. This work discusses the setup and results of a test program carried out to determine the effectiveness and impact of this cooling effect as it pertains to LH_2 upper stage tanks. A vertical-cylindrical liquid nitrogen (LN_2) calorimeter test instrument acted as the upper stage analog. The cold-mass was wrapped with two layers of 10 mm thick aerogel blanket material, with and without aluminum heat shields depending on the test, and interspersed with numerous thermocouple temperature sensors. Gaseous argon was used as a stand-in for air as the condensable background gas. The test procedure mimicked vehicle cryo-loading/stabilization, and ascent phases, with the ascent phase accomplished using parallel vacuum pumps. Results show that the desorption cooling effect was enough to not only eliminate the heat load on the LN_2 cold-mass entirely, but further refrigerated the liquid below its boiling point.

Nomenclature

Units

K	Temperature, Kelvin
sccm	Mass Flow Rate, standard cubic centimetres per second
torr	Absolute Pressure
ΔT	Temperature Difference

Abbreviations

KSC	Kennedy Space Center
LH_2	Liquid Hydrogen
MLI	Multi-Layer Insulation
NBP	Normal Boiling Point
SOFI	Spray-On Foam Insulation
LN_2	Liquid Nitrogen
LAr	Liquid Argon
C-100	Cryostat-100 Test Instrument
MFC	Mass Flow Controller

1. Introduction

Owing to its superior specific impulse, liquid hydrogen (LH_2) has been the rocket fuel of choice since the dawn of human space flight, especially for upper stages. Vehicles such as the Centaur upper stage, 2nd and 3rd stages of the Saturn V moon rocket and Space Shuttle employed the fuel, and today it powers numerous private vehicles, as well as both stages of NASA's Space Launch System and the European Space Agency's Ariane 6 launcher. Utilization of LH_2 however, presents various challenges associated with operating systems at deep cryogenic temperatures. With a normal boiling point (NBP) close to 20 K, LH_2 vessels and piping will readily liquify the surrounding air and accumulate water-ice when filled for launch if not properly insulated, which itself poses a safety risk, but also introduces a large heat load on the valuable liquid propellant that translates to high boiloff rates.

For these reasons, some means of insulating the LH_2 tanks of flight vehicles is always necessary. However, unlike first stages that burn the majority of their propellant while attempting to escape the Earth's atmosphere, upper stages, which, as previously mentioned, are the primary candidates for usage of LH_2 fuel, must manage and utilize the hydrogen both on the ground and in the vacuum of space. This point is crucial because thermal insulation systems such as Spray-On Foam Insulation (SOFI) that work well in the ambient pressure environment present during LH_2 fill and ground hold phases of a launch countdown are significantly different than those that are aimed at providing high performance in a vacuum such as Multi-Layer Insulation (MLI). Additionally, any insulation system applied to the outer, windward-facing side of a tank must survive ascent to orbit without being destroyed by aerodynamic loads and/or heating, or vibration, and be of sufficiently low density as not to negatively impact the payload mass capacity.

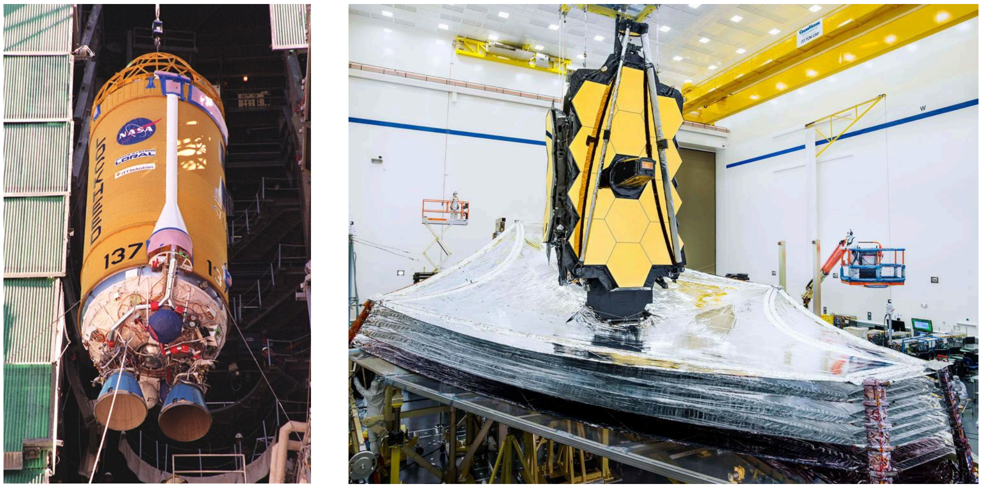

Figure 1. Characteristic Orange SOFI Applied to Windward-Facing Side of a Centaur Upper Stage (left); MLI Configuration of the James Webb Space Telescope

The combination of these factors makes the design and execution of windward-facing cryogenic thermal protection systems for launch vehicles one of the most challenging insulation problems in all of engineering. As a result, much of the effort over the last 60+ years has focused on upper stage insulation systems optimized for pre-launch phases, meaning that on-orbit LH_2 operational timelines are constrained to mere hours in order to accommodate the large boiloff rates. The significance of this issue was pointed out in a 2016 paper by Bernard Kutter of United Launch Alliance (ULA) where improving the on-orbit hold-time of LH_2 upper stages from hours to weeks was acknowledged as critical to facilitating a robust future space economy under their Cislunar-1000 architecture [1].

Combining insulations with acceptable ambient pressure and high vacuum performance into a synergetic system that meets the requirements listed above is extremely difficult. One approach that has been explored by the Cryogenics Test Laboratory at NASA Kennedy Space Center (KSC) hinges on the use of robust, flexible aerogel blanket material. Aerogel blanket has superior performance in an ambient pressure environment, with an effective thermal conductivity roughly 33% lower than SOFI [2], and, by virtue of its intrinsic robustness, can provide a means of protection during ascent for layers of more fragile MLI that can combat radiation heat leak once on-orbit. An additional feature of aerogel stems from its nano-porous structure and, by extension, extremely high surface area (~1000 m^2/g): at cryogenic temperatures it becomes an excellent adsorbent, and will readily uptake large amounts of background gas such as air (a detailed explanation into the physics of adsorption is beyond the scope of paper, but can be found in Boer [3]). Even more interesting perhaps, if adsorbed aerogel is rapidly exposed to a vacuum, as would be the case on the windward-facing side of a launch vehicle, the trapped gas will escape (i.e. desorb), producing a cooling effect as the molecules carry heat away from the material in response to the pressure change. Additionally, it is hypostasized that capillary evaporation and/or sublimation within the aerogel pores may also contribute to the cooling effect; however, this is not well understood or substantiated at this time. The cooling phenomenon is apparent in Figure 2, where a sample of aerogel blanket material from Aspen Aerogels was instrumented with thermocouples, saturated with liquid nitrogen (LN_2) at 77 K, and then pumped down in a vacuum chamber. The blanket temperature responded dramatically and immediately to the drop in pressure, reaching the triple point of nitrogen in roughly 1 minute, and continued to fall , eventually plateauing below 55 K—over 20 K below the NBP.

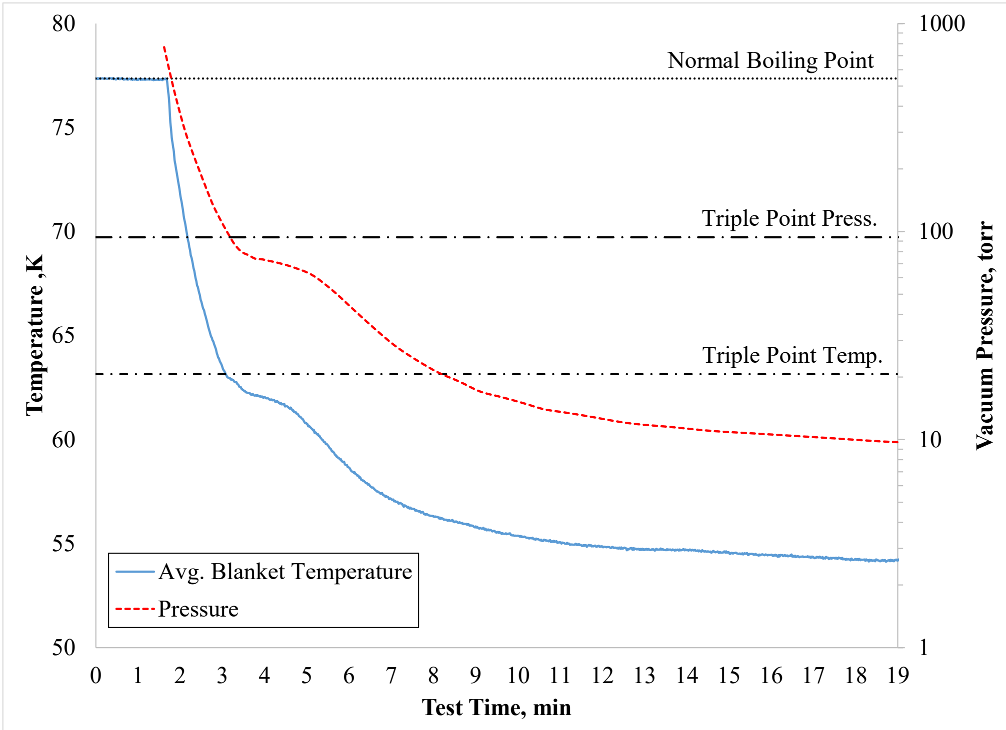

Figure 2. Vacuum-Induced Cooling in Aerogel Blanket Sample Using Liquid Nitrogen

In the current work we explore some of the ramifications of vacuum-induced cooling in aerogel blanket material as it pertains to the application of LH_2 upper stages; in particular, whether it can be exploited to provide passive cooling directly to the LH_2 tank during ascent and early orbital operations in order to reduce or eliminate boiloff. Using the Cryostat-100 (C-100) test instrument [4], a vertical-cylindrical liquid nitrogen calorimeter, a situation analogous to an actual launch was created by substituting gaseous argon for air, filling the cold-mass (i.e. the upper stage tank analog) with LN_2, and pumping down the vacuum chamber to simulate ascent and orbit—although, aero-related factors and precise depressurization profiles were not accounted for. As the liquefaction point of argon is roughly 10 K above that of nitrogen, it could act as a suitable condensable background gas, imitating the true combination of LH_2 and air for an upper stage on the launch pad—it is acknowledged of course that the ΔT between the NBP's of hydrogen and air is much larger than nitrogen and argon, roughly 58 K versus 10 K, however, this was a necessary concession due to safety and other practical factors, and was believed to still yield valuable results. The cold-mass of C-100 was wrapped with two layers of 10 mm thick Cryogel® aerogel blanket material from Aspen Aerogels, with and without aluminum heat shields depending on the test, and interspersed with numerous thermocouple temperature sensors. Aerogel blanket insulation and its application in LH_2 systems is discussed, and the results of the LN_2/argon combination "launch test," are presented.

2. Aerogel Blanket Insulation

Development of aerogel blanket material began in the 1990's by NASA and its partner Aspen Systems (now Aspen Aerogels) to address the need for cryogenic insulation systems with increased thermal performance [5]. By the mid-2000's, Aspen had commercialized the product, and today offers a variety of material options for both low and high temperature applications.

Fundamentally, aerogel blanket is a composite material, consisting of a non-woven fiber matrix batting that has been completely encapsulated with silica aerogel through the sol-gel process and supercritical drying. Silica aerogel is inherently brittle and will easily fracture in monolithic form. However, as a composite the batting provides structure, analogous to rebar in concrete, resulting in a robust, flexible product that can be securely wrapped around objects and easily cut into complex shapes. Additionally, the blankets are treated during production to make them super-hydrophobic.

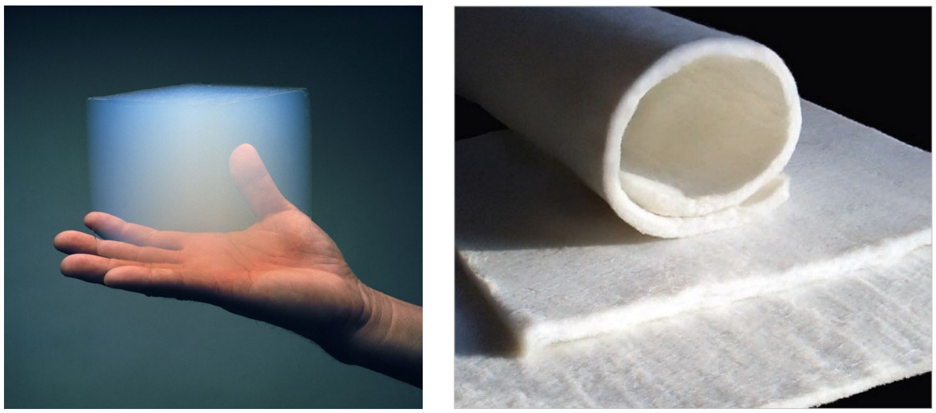

Figure 3. Silica Aerogel Monolith (left); 10 mm Thick Cryogel® Product from Aspen Aerogels (right)

2.1 Thermal Performance

A thorough examination of the cryogenic thermal performance for various insulation systems, including aerogel blanket, was presented by Fesmire [6]. Figure 4 compares the effective thermal conductivity for a selection of insulation systems relevant to the current work for boundary temperatures between 78 K and 293 K, and over a vacuum range from 0.001 millitorr to ambient pressure.

Figure 4 clearly shows the improvement in ambient pressure performance for aerogel-based insulation systems over SOFI, and that benefit only increases with decreasing pressure—at 760 torr, Cryogel® is around 33% better, but at 0.1 millitorr that increases to 80%. Another fact revealed by Fig. 4 is that the inclusion of even a small number of thermal radiation shields has a dramatic effect on the vacuum performance of the overall insulation system, which emphasizes the importance of incorporating them into LH_2 upper stage cryogenic thermal protection systems to increase on-orbit hold-times. At 0.1 millitorr the A193 aerogel paper/MLI hybrid specimen, which only had four double-aluminumized Mylar shields, including one applied directly to the stainless steel cold-mass, had an effective thermal conductivity over two orders of magnitude lower than SOFI, and resulted in a 25x reduction in heat flux. Such an improvement in performance could result in, for example, a reduction in on-orbit LH_2 boiloff rate for the Centaur upper stage from 4.1% per day [7] to around 0.16% per day.

An obvious disparity between the data presented in Fig. 4 and the application to LH_2 systems is the much higher cold boundary temperature employed during the LN_2 boiloff calorimetry testing that generated the curves. However, as the absolute values for a given insulation system will undoubtedly change for a boundary condition of 20 K versus 78 K (refer to Ref. 6 for a method to estimate the impact) the relationship between different insulation systems is expected to remain unchanged. Therefore, performance comparisons between different insulations at 78 K, as was done here, should transfer down to 20 K as well, whereas the effective thermal conductivity of a particular option would change.

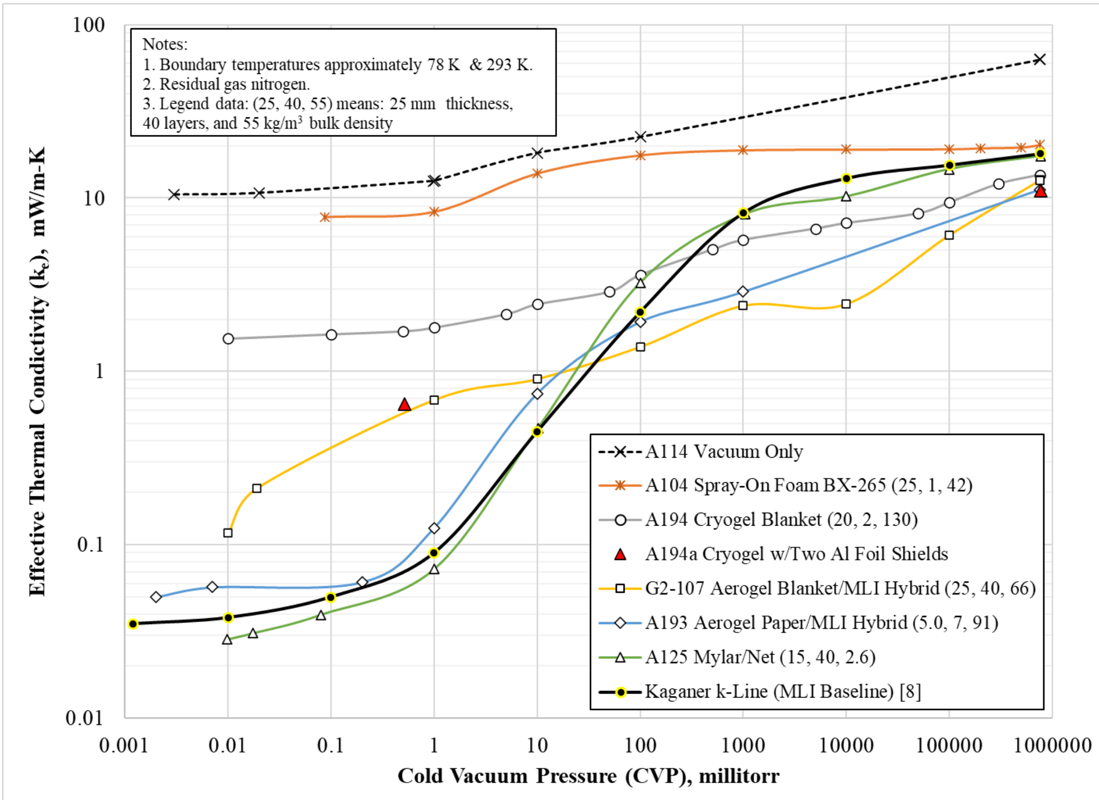

Figure 4. Thermal Performance Comparison of Various Cryogenic Insulation Systems Between 78 K and 293 K (refer to ASTM C1774 for a full explanation of nomenclature and test method)

2.2 Application in Current Liquid Hydrogen Systems

Apart from the unique application of LH_2 tanks for space launch vehicles, rarely are LH_2 systems designed to forgo the aid of vacuum in their insulation system approaches. Virtually all LH_2 storage tanks, transfer piping, and components are vacuum-jacketed with MLI to control heat leak and eliminate air liquefaction. Only for interface points that are intended to be connected/disconnected, or reconfigured on a regular basis do uninsulated surfaces tend to come into play; in which case the heat load can be extremely large, and the methods and options to apply external insulation materials are limited. Many times, these surfaces are simply left exposed, and provisions such as drip pans are put in place to safely manage the liquid air.

Due to the nature and diversity of the type of LH_2 ground support hardware and testing facilities at KSC, there are numerous instances of uninsulated components employed. In some cases, the combined heat load associated with these components was high enough to negatively impact test operations and endanger the success of testing campaigns, which drove the need for an externally applied insulation solution. One such option, developed by the Cryogenics Test Laboratory, is the aerogel-based Layered Composite Insulation (LCI)—most notably the "extreme" variation (LCX) made for non-vacuum, outdoor environments [9]. Aerogel blanket is typically used as the primary insulation material in the LCI family of thermal insulation systems; and for LCX, blanket layers are interleaved with compressible radiation barriers to form a robust, yet compliant product that that is both hydrophobic and unaffected by thermal expansion/contraction of the protected hardware—all attributes that lend themselves well to the application of upper stage LH_2 tanks. Additionally, LCX has been successfully implemented on numerous bare LH_2 valves, flanges, piping, and other components at KSC, and was proven effective at reducing heat leak and liquid air formation over numerous LH_2 flow tests. Figure 5 shows representative LCX stack-ups and installation photos on an uninsulated LH_2 valve and fill and drain ports at KSC.

Although dissimilar in many ways to an LH_2 upper stage tank, these real-world examples demonstrate how aerogel-based, externally applied insulation systems can be successfully employed in LH_2 applications.

Figure 5. LCX Sample Stack-Ups with Three Layers of Aerogel Blanket (upper left); LCX Insulated LH_2 Valve (foreground) and Uninsulated Unit (background) (lower left); LCX Installed on LH_2 Fill & Drain Ports (right)

3. Passive Cooling Test Setup & Method

As was stated previously, the core point of the passive cooling lab test was to imitate, as closely as practically possible, the situation present for an insulation system that is externally applied to the windward-facing side of an LH_2 upper stage tank during cryo-loading and launch. Fundamental to this end was to have a vertical-cylindrical cryogenic tank that could be wrapped with insulation and pump-down to vacuum—both features that the C-100 instrument provided—and a condensable background gas to mimic the LH_2/air combination, which was achieved through the use of LN_2/argon.

3.1 Overall Test Setup

Figure 6 shows a high-level functional diagram of the passive cooling test setup, and consisted of five main components: 1. A 180 liter liquid argon (LAr) dewar used to supply gas to the C-100 chamber, and chosen in place of high-pressure gas bottles to ensure an adequate gas source was always available during the test; 2. An 85 liter buffer volume vessel; 3. A mass flow controller (MFC) used to meter the flow of argon into the system based on a C-100 chamber set pressure; 4. The standard C-100 lab instrument with upper and lower guard chambers protecting a middle test chamber and internal heater sleeve; and 5. A set of three vacuum scroll pumps—one Leybold brand SC15D model, and two ANEST IWATA brand ISP-90 models—configured in parallel. Also shown are nitrogen mass flow meters (MF1, MF2 & MF3) used to measure the boiloff rate from each of the three LN_2 chambers; LN_2 filling ports for filling from portable hand dewars; data acquisition system (LabVIEW), thermocouple locations, isolation valves (V1, V2 & V3), and a vacuum pressure transducer (PT). Figure 7 shows the actual hardware configuration, with and without the cold-mass removed. The test specimen consists of two 10 mm thick Cryogel® blanket layers, and the left-most picture in Fig. 7 includes the aluminum foil shields, with the outer shield clearly visible. Both shields consisted of a single 0.127 mm thick foil sheet, wrapped snuggly around the corresponding aerogel blanket layer, and secured with a single strip of aluminum tape longitudinally down the seam to form a radially sealed gas barrier (i.e. gas was still able to access the aerogel blanket layers from the open ends). This configuration was chosen over more efficient venting perforated aluminum sheets or aluminized Mylar because it was thought to have the most impact on the rate argon uptake in the specimen.

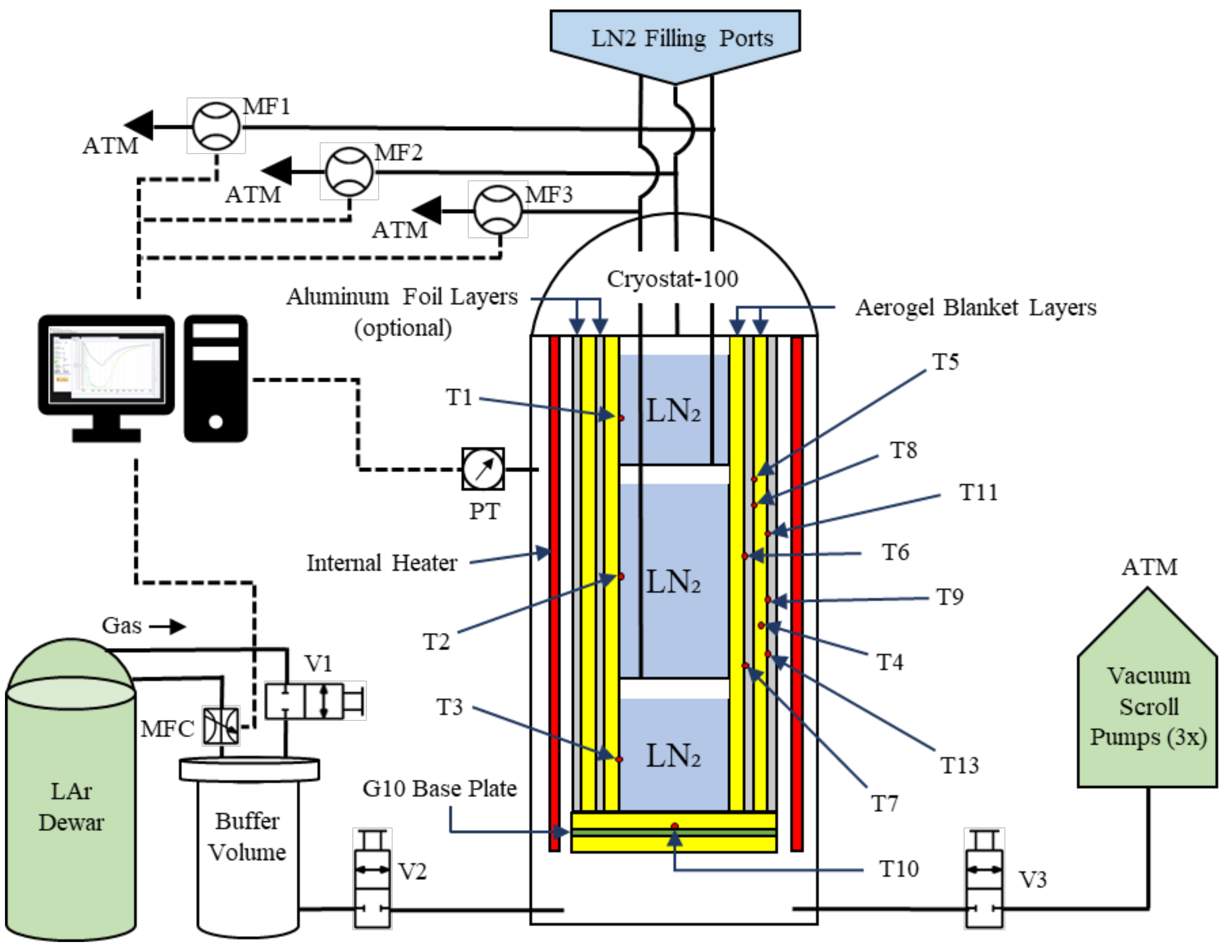

Figure 6. Functional Diagram of the Passive Cooling Test Setup

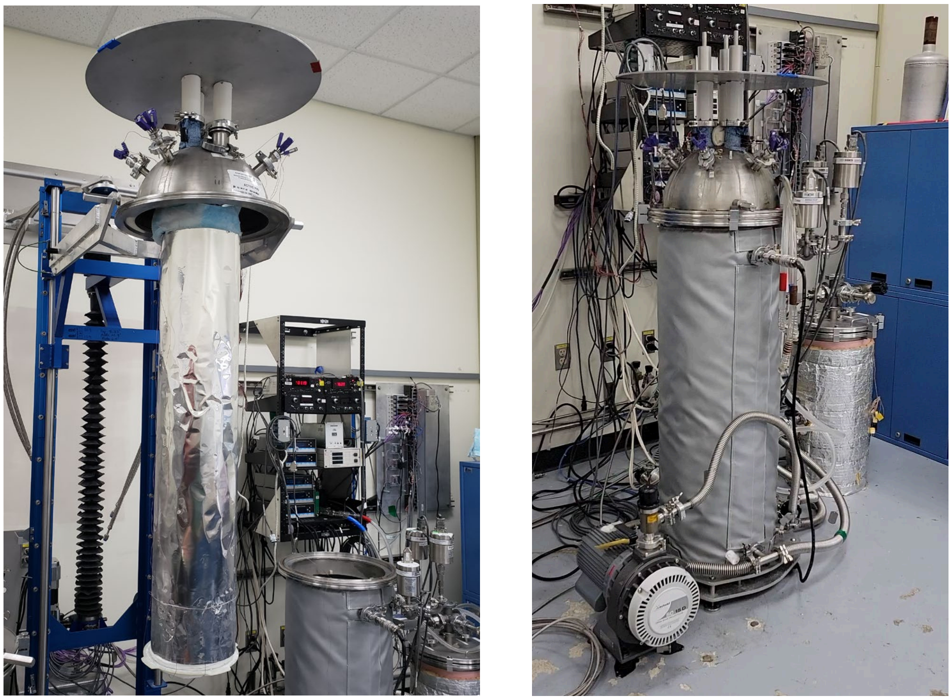

Figure 7. Passive Cooling Test Hardware Configuration: Cold-Mass with Cryogel® & Aluminium Foil Specimen (left); Assembled Cryostat-100 Calorimeter Showing One of the Vacuum Scroll Pumps (foreground) and Buffer Volume (background) (right)

3.2 Fluid Delivery Systems

Delivery of gaseous argon to the system originated from the 24 bar LAr dewar, and after passing through a gas regulator to reduce the pressure to around 3.5 bar, the argon flow divided into two pathways. The first path fed the MKS brand GM50A MFC, which autonomously maintained a previously set pressure level of 760 torr in the C-100 vacuum chamber, and the second led to a 12.7 mm shut-off valve (V1) used to manually regulate the buffer volume gas intake as a contingency in case the MFC could not maintain the set pressure. LN_2 was filled by-hand via “stinger-type” fill funnels, and boiloff gas was routed from the feedthrough ports on the top of the chamber to the three mass flow meters via flexible Tygon® tubing.

3.3 Instrumentation

Figure 6 calls out fifteen thermocouples (type-E) distributed within the different layers of insulation and attached to the cold-mass. The thermocouples can be split into four general groups by location. Group 1 are the cold-mass temperatures T1, T2, and T3, and are each secured directly to the stainless-steel cold-mass wall. Group 2 consists of T5, T6, and T7, and were located between the two primary layers of the insulation material (in the case of testing with the two aluminum foil barriers, thermocouple placement was consistent with the configuration shown in Fig. 6). Group 3 was positioned in the outermost layer of insulation and includes T8, T9, T11, and T13. Lastly, Group 4 consists of T10, located at the very bottom of the C-100 cold mass between the first aerogel layer and G-10 base plate. Nitrogen mass flow meters were MKS brand M10MB models, with ranges of 10,000 sccm on the top and bottom guard chambers, and 50,000 sccm on the test chamber; and the vacuum pressure transducer was a 1000 torr Baratron® capacitance manometer from MKS. All temperature, pressure, and flow data were captured by a custom LabVIEW program, which also handled control of the argon mass flow controller.

3.4 Testing Rationale & Procedure

As the intent of the test program was to create an analogous situation to a launch of an LH_2 upper stage, the test was broken into two phases: 1. A cryo-loading/stabilization phase where the chamber would be maintained at 760 torr argon while the cold-mass was cooled down to LN_2 temperature, and then the system would be allowed to stabilize (i.e. when the argon flow through the MFC ceased and the thermocouples reached constant temperatures); which would be followed by 2. An ascent phase where the chamber would be quickly pumped down to vacuum using the parallel scroll pumps.

Prior to initializing a test, the system was evacuated by the vacuum pumps to eliminate any residual gases inside the vacuum chamber and lines, and then backfilled with argon to 760 torr. The cryo-loading/stabilization phase then commenced with LN_2 filling of all three liquid chambers in tandem. The initial, transient cooldown process tends to take a considerable amount of time with the C-100 instrument due to the limited vent paths caused by the configuration of the fill tubes and feedthroughs, so fill level in the funnels was maintained until the cold-mass temperatures flat-lined at their minimum values, and then the chambers were refilled periodically if necessary. Once stabilization occurred, testing would transition into the ascent phase by isolating the vacuum chamber from the buffer volume by closing valve V2, and then the vacuum scroll pumps turned on to rapidly evacuate the chamber.

4. Test Results & Discussion

Figure 8 presents the results of the cryo-loading/stabilization test phase with two layers of 10-mm Cryogel® aerogel blanket material, without aluminum shields; while Figure 9 shows the ascent phase results.

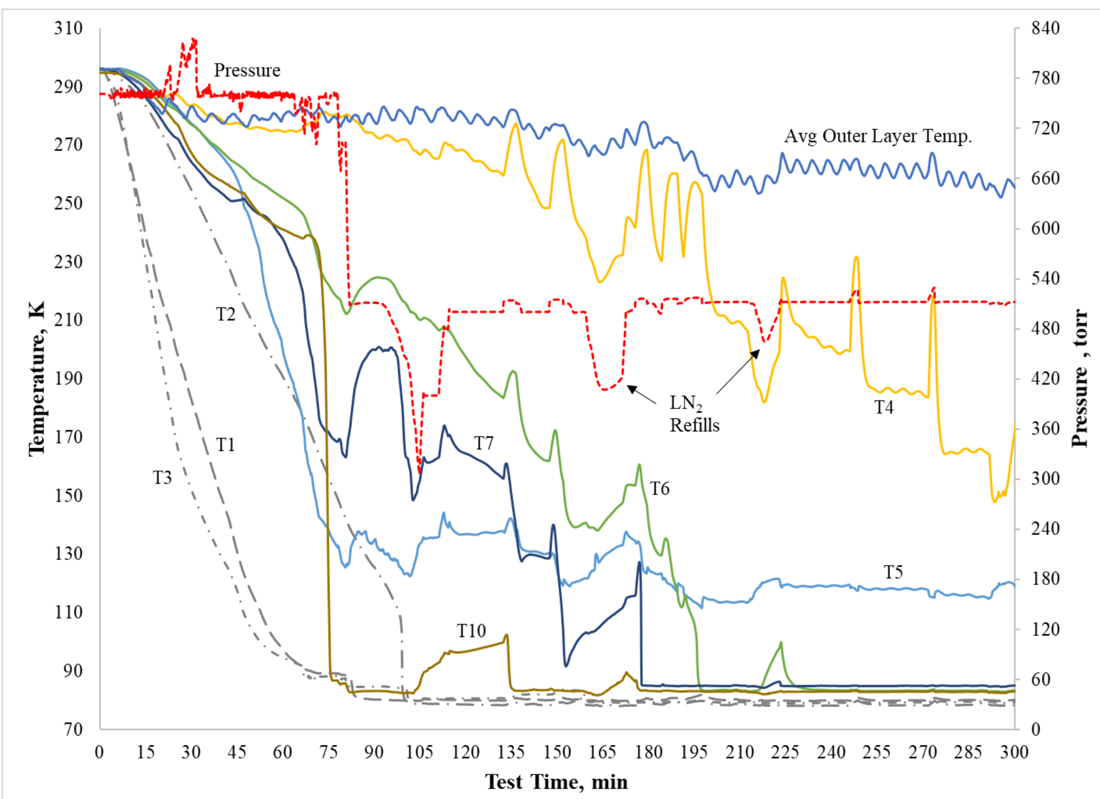

Figure 8. Results of Cryo-Loading/Stabilization Test Phase

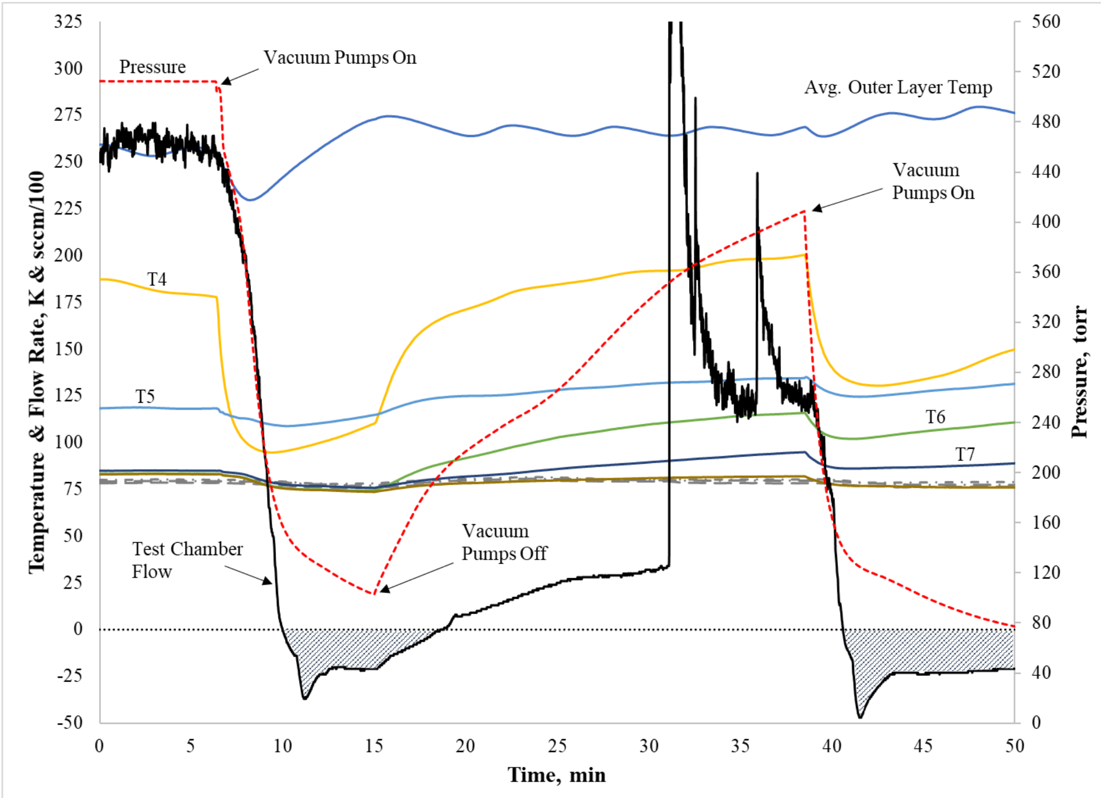

Figure 9. Results of Ascent Test Phase Showing Negative Test Chamber Flow (shaded regions)

4.1 Discussion

Figure 8 reveals several interesting features during the cryo-loading/stabilization phase of testing. The average outer layer temperatures (T9 and T11) were maintained at a relatively warm temperature throughout the testing (fluctuations are in response to the heater controller), however, as the cold-mass—represented by the three, gray, dashed lines, T1, T2 & T3—approached the NBP of argon (87 K) there was a dramatic decrease in temperatures within the aerogel blanket layers, with T10 making an apparent instantaneous jump to the NBP around the 75-minute mark. This coincided with an abrupt drop in pressure as well, from 760 torr to around 512 torr, followed by sudden increase in layer temperatures T5, T6, and T7 from about 80 to 95 minutes. Interestingly, the argon mass flow controller was not inputting mass into the chamber during this time. It is believed that this increase in temperature was due to the sudden inrush through the blanket, of warm argon that already existed within the chamber. Soon thereafter the pressure dropped suddenly again, spiking at around 105 minutes before the flow controller attempted, unsuccessfully, to bring the pressure back to 760 torr

Following this initial transient period, the mass flow controller continuously introduced argon into the system, but was unable to increase the pressure above 512 torr—of particular note, and undoubtedly not a coincidence, 512 torr is roughly the triple point of argon (516.8 torr and 83.8 K). During this time the layer temperatures also continued to fall as the blanket adsorbed large amounts of argon, until most of the temperatures reached ~83 K. It was attempted several times to increase the pressure back to ambient by opening the argon bypass valve (V1) and quickly introducing a large amount of gas into the chamber. These attempts show up as numerous small blips in the pressure and temperature data. However, it was obvious that the pressure could not be increased using the gas management system employed, and there were fears that the issue was due to argon being liquefied on some uninsulated cold-mass surfaces, which would ultimately accumulate toward the bottom of the cold-mass and drip down onto the vacuum chamber—there was evidence of this during the test as the base of the vacuum chamber began to frost over at one point, and was realized during follow-on testing discussed in the next section. Hence, it was decided around the 285-minute mark to turn off the mass flow controller and allow the system to stabilize in preparation for the ascent phase of the test.

Rapid pump-down of the system, shown in Fig. 9, yielded some dramatic and unexpected results. Prior to turning the vacuum pumps on around the 7-minute mark the test chamber flow rate was measured to establish a baseline heat load. From 0 to 5 minutes the average flow rate was 25,992 sccm (0.534 g/s), which translates to a heat load of 106.4 W. Once the baseline was established, the vacuum pumps were turned on to mimic the ascent of an upper stage, which initiated an immediate and dramatic drop in the test chamber flow, eventually reaching zero around the 10-minute mark and even going negative for a time (shaded region) before the pumps were isolated and the pressure began to climb again—and, although not shown in Fig. 9, both the top and bottom guard chamber flows also went negative. As can be seen later in the test, this process was duplicated beginning around 40 minutes.

As the flow rate is a direct result of heat ingress into the test chamber, reversal of the flow can only be achieved by removing heat directly from the cold-mass—or, in other words, by providing refrigeration power to cool the LN_2 below its boiling point—and can only be a result of the endothermic cooling effect afforded by the aerogel blanket, as there was no other source of sub-LN_2 temperature heat removal in the system. In addition to the flow meter data, test personnel verified reversed flow in the test and guard chambers by briefly sealing off the fill ports and witnessing the vacuum created. Flow was negative for roughly 8.5 minutes the first cycle, with a maximum rate of -3672 sccm, and was negative for much longer in the 2nd cycle due to the pumps being left on, with a maximum negative flow rate of -4727 sccm. Huge spikes in the flow beginning around 30 minutes were witnessed in each chamber and in every test, and were believed to be due to the sudden boiling of a small amount of liquid air that was liquefied inside the chambers while the flow was negative.

A rough estimate of the refrigeration power (i.e. passive cooling) provided to the test chamber by the aerogel blanket can be obtained by assuming that the negative flow rate of air was also a liquefaction rate, hence the heat removal can be calculated by multiplying this rate by the heat of vaporization of air at ambient pressure—205 J/g for an 80% nitrogen, 20% oxygen mixture [10]. Using this method, for the first pump-down cycle the maximum desorption cooling power was around -16 W, and was -20 W for the second cycle. Assuming this power was distributed evenly over the entire surface area of the test chamber yields peak fluxes of roughly -31 W/m^2 and -39 W/m^2 for the first and seconds cycles respectively.

Figure 10 shows the first pump-down cycle presented in Fig. 9, and zooms in on the cold-mass temperatures (T1, T2, & T3). During the period of negative pressure the blanket temperatures clearly fell below the LN_2 cold-mass temperatures, which is consistent with the reversed heat flow necessary to create the reversed test chamber flow rate. The lowest temperature recorded was 74 K, on T10, which is roughly 3 K below the boiling point of nitrogen, and 10 K below the freezing point of argon, revealing the substantial passive, vacuum-induced cooling power afforded by saturated aerogel blanket. Additionally, the lowest vacuum pressure achieved was still orders of magnitude higher than would be seen on an actual ascent of an upper stage, which would most likely result in an even higher degree of passive cooling than was witnessed during this testing program.

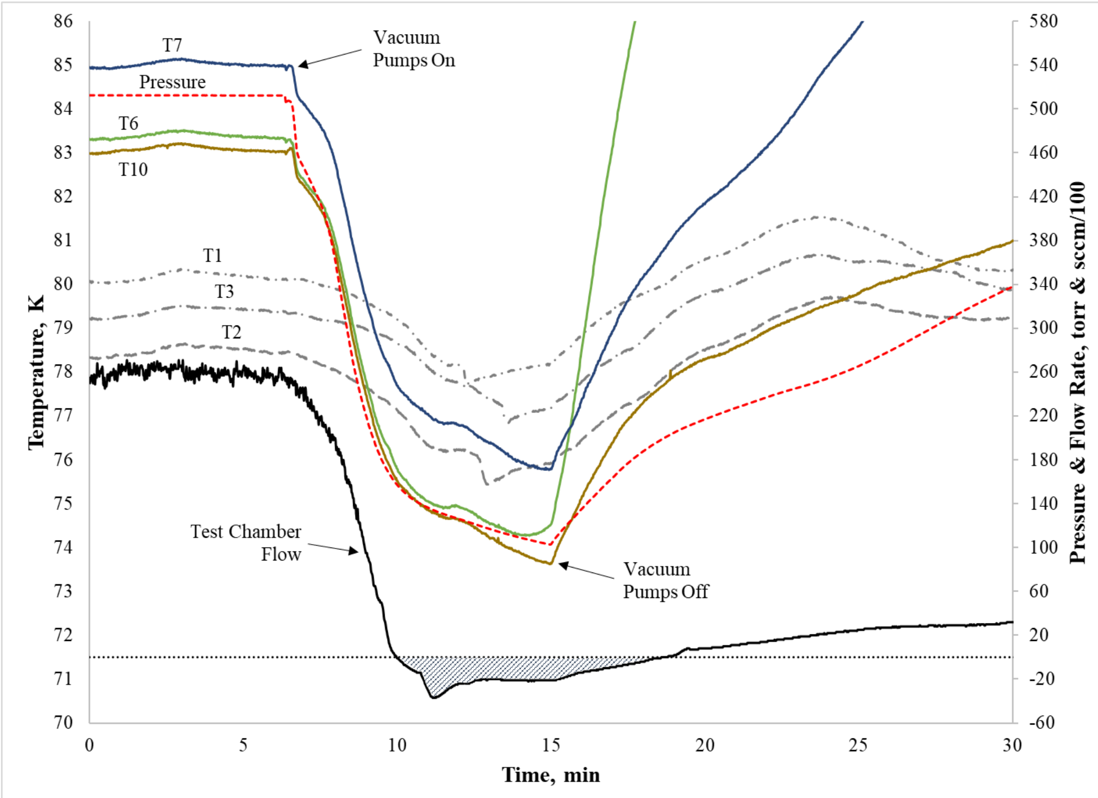

Figure 10. Zoom-In on Lower Temperature Region from the Ascent Test

4.2 Inclusion of Aluminum Heat Shields

Figures 11 through 13 show the results of an equivalent test program carried out on the specimen after installing two 0.127 mm thick, solid aluminum foil shields. Similar ascent results were obtained, with a maximum negative flow rate of -4543 sccm witnessed during pump-down. However, the cryo-loading/stabilization phase was considerably different. Unlike the prior test with only two aerogel blanket layers, inclusion of the shields allowed the gas management system to keep and maintain the argon pressure at the setpoint of 750 torr inside the vacuum chamber throughout most of the test phase. As before though, the system did not self-stabilize, and required a continuous influx of argon gas to maintain the pressure. This fact eventually led to the realization of the fear discussed previously: an apparent over-saturation of the aerogel blanket on the bottom of the cold-mass due to argon liquefaction, and dripping of liquid onto the vacuum chamber floor. This free liquid quickly vaporized upon contact with the warm chamber wall, raising the pressure above atmospheric and venting though a vacuum relief valve at roughly 860 torr. This event can be seen in figure 11 beginning around 155 minutes. During this period, the mass flow controller was turned off and the chamber allowed to vent back down to the MFC set pressure. The MFC was then powered back on and immediately began to introduce large quantities of argon gas into the chamber, creating a noticeable spike in the pressure around 175 minutes before settling back down to a stable pressure around 768 torr. Ultimately, to prevent further liquefaction of argon, the MFC was again turned off and the pressure allowed to stabilize—predictably, again to around 500 torr—prior to transitioning into the ascent test phase.

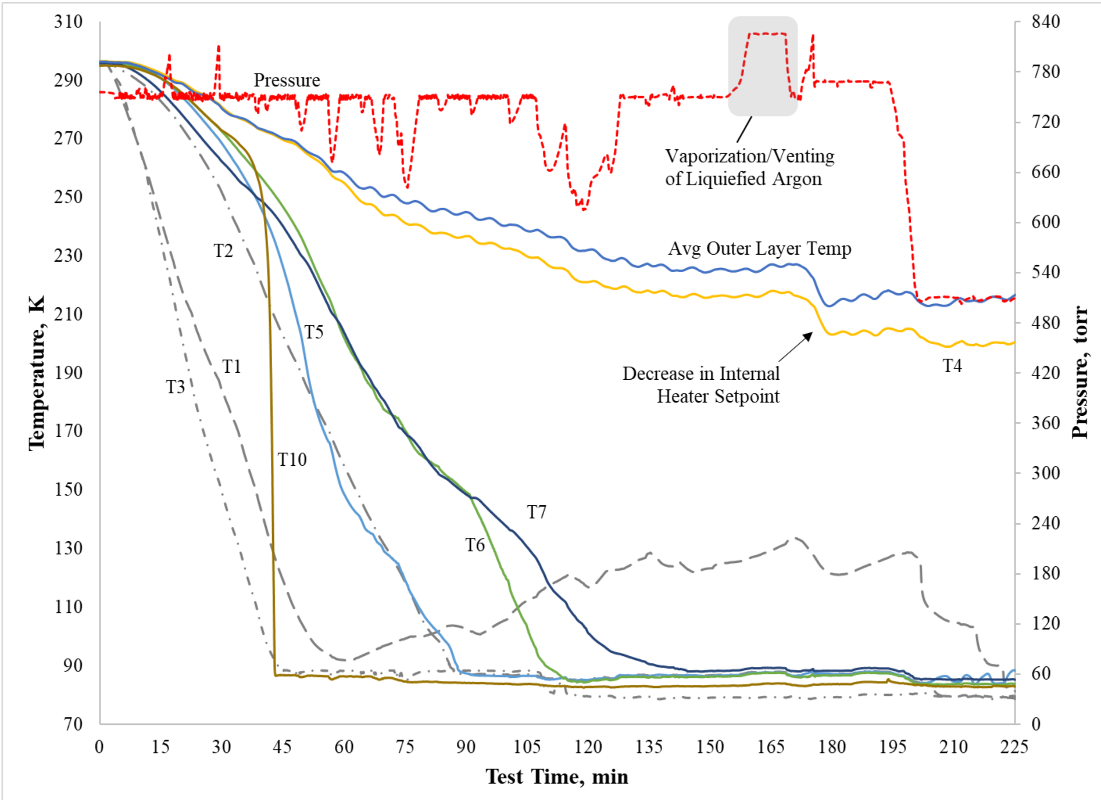

Figure 11. Results of Cryo-Loading/Stabilization Test Phase with Aluminium Shields

Another notable difference between the two cryo-loading/stabilization tests was the much lower average outer layer temperature seen in the specimen with aluminum shields. Cycling of the internal heater is evident in both cases, however, the temperature for the specimen with shields plateaued around 35 K lower than without shields. In response to the realization that the outer layer temperature could not be increased to a similar level as the previous test, a real-time decision was made, around the 170-minute mark, to reduce the heater setpoint by 25 K, back to ambient (293 K). This decrease triggered a precipitous fall of the outer layer temperature another 10 K, and is called out in figure 11. An examination of the heater temperatures (not shown in the figures for sake of clarity) revealed only a slightly higher (roughly 10 K) maximum for the test with aluminum shields. Hence, it stands to reason that the inclusion of the outer-most aluminum foil layer provided a substantial thermal resistance, as T9 and T11, the average of which constitute the outer layer temperature, were located on the backside of the foil, in between it and the first aerogel blanket layer.

Although the system did not achieve the desired stabilization at ambient pressure in either test without the continued introduction of make-up gas, it is obvious from figure 11 that the addition of radially sealed barriers had a significant impact on the rate at which the aerogel blanket adsorbed the background gas. This makes intuitive sense, as the shields dramatically reduced the surface area accessible to the gas by only allowing it to access the blanket axially from the ends of the test specimen. This sample configuration was also considered to be more “flight-forward” due to the aluminum barrier material. In a sense, the total aerogel blanket & aluminum shield insulation system was a type of robust MLI—exactly what would be necessary to address the ground, ascent, and orbital phases of an actual LH_2 upper stage flight.

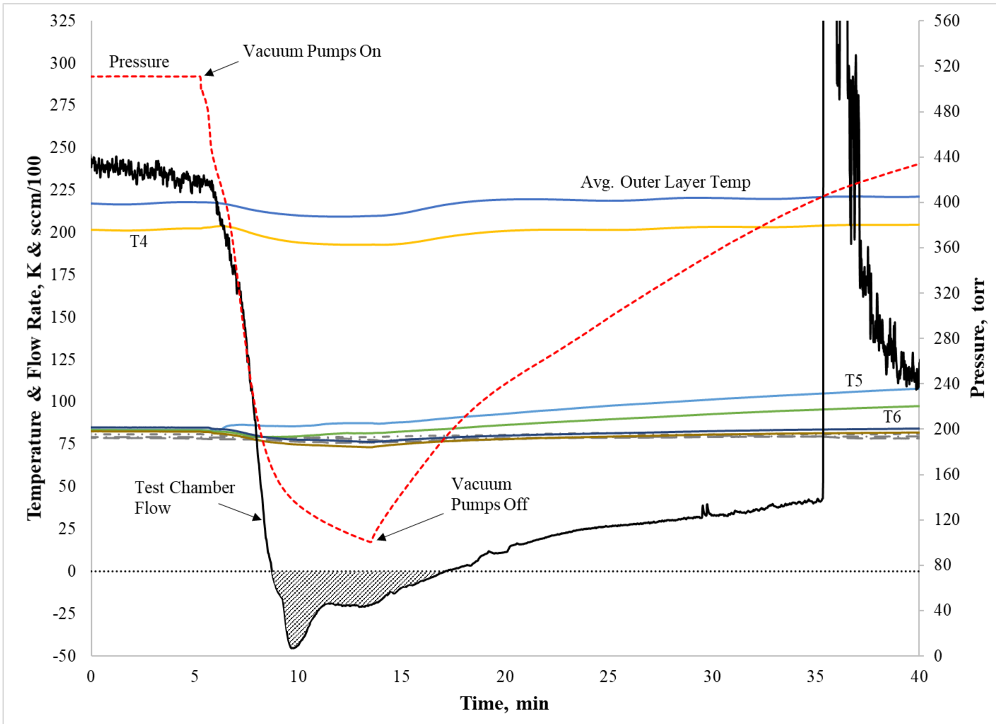

Figure 11. Results of Ascent Test Phase with Aluminium Shields

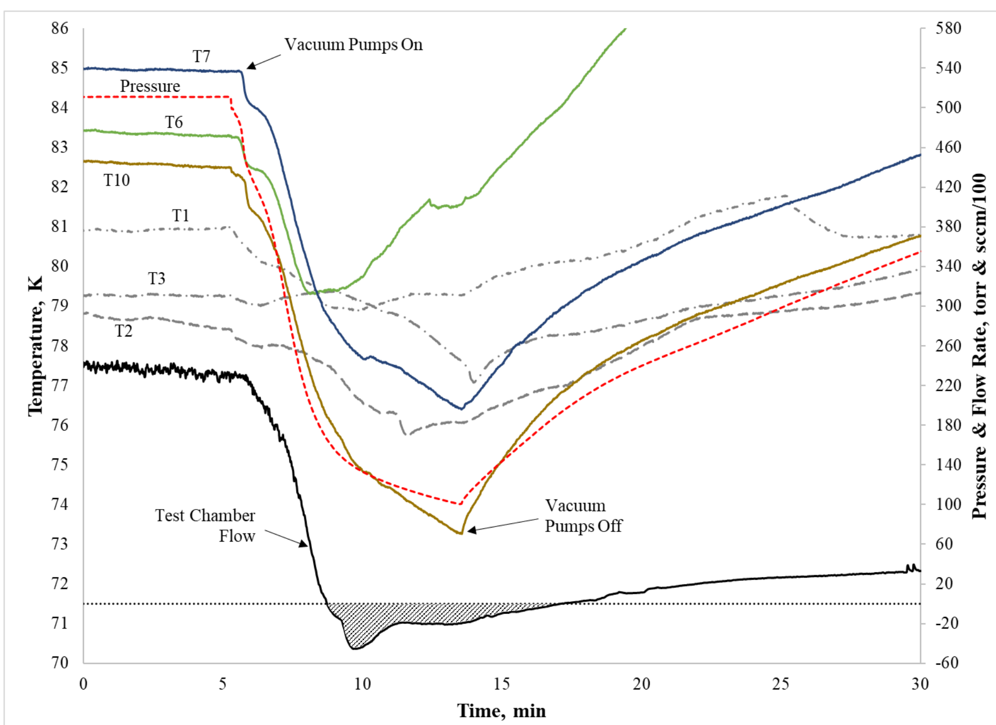

Figure 12. Zoom-In on Lower Temperature Region from the Ascent Test with Aluminium Shields

The additional vacuum thermal performance afforded by the two shields was also examined via a standard C-100 boiloff calorimetry test and is apparent from the data comparison shown in Fig. 4. At 0.5 millitorr the shielded version (test A194a) outperformed the non-shielded version (test A194) considerably, reducing the effective thermal conductivity by 62%.

It should be noted, although more flight-forward in intent, this specimen configuration cannot not be taken to be at any acceptable level of maturity to meet the technical requirements for an actual flight vehicle application. A multitude of additional considerations must be addressed—some of which will be discussed in the following section—when designing and implementing an actual flight version beyond those examined in this work.

5. Challenges Related to LH_2 Upper Stage Applications

The primary purpose of this work was to examine a particular aspect related to aerogel-based insulation—vacuum-induced, passive cooling—as it pertains to LH_2 upper stage tanks. However, there are many technical, manufacturing, and operational challenges that need to be addressed to facilitate the usage of such insulation systems on actual upper stage tanks. Some key examples are touched-on below.

First and foremost is the large mass penalty that must be paid due to the uptake of condensable background gas by the aerogel insulation during cryo-loading on the ground. Although this mass would be paid back in the form of passive cooling during ascent and early orbital operations, it would directly add to the launch mass of the vehicle and negatively impact performance and/or payload mass fraction. Without extensive design and testing on relevant scales and actual use conditions it remains to be seen whether this trade-off could ultimately be beneficial to upper stage mission profiles.

Another issue is LH_2 tank pressure control, both internal and external. As was demonstrated by the testing presented in this work, the passive cooling provided to the tank by the aerogel blanket was sufficient to refrigerate the liquid nitrogen below its boiling point, resulting in a negative test chamber flow rate. In a closed volume such as an LH_2 upper stage tank this could result in a sub-atmospheric pressure condition inside the vessel if the in-flight pressurization system was inadequate. As most flight tanks are built with low factors of safety to reduce mass, and rely on a consistent positive pressure to provide overall structural strength to the vehicle, they would most likely not tolerate even a moderate inverted pressure condition. In order to accommodate the passive cooling, in-flight pressurization systems and operational control schemes would most likely need to be upgraded. Similarly, it is possible that, if the design of the insulation system does not properly allow the desorbed gas to vent during flight, pressure could potentially build-up within the layers. If the insulation system was strong enough to withstand the pressure, an external force would be applied to the outside of the LH_2 tank, causing a similar situation as negative internal pressure; or, if not, the insulation system would burst and be destroyed. Most likely this issue could be addressed by employing properly designed perforated thermal radiation shields and/or other protective layers within the overall insulation system. Such an approach is common practice for MLI blankets protecting spacecraft housed within a launch vehicle fairing.

Stabilization of the insulation system during and after cryo-loading also poses a potential challenge. This issue is commonly referred to as "cryo-pumping" and is the uncontrollable and continuous liquefaction of condensable background gas on a cold tank surface. There is anecdotal evidence to suggest that aerogel insulation materials prevent cryo-pumping even when protecting surfaces at LH_2 temperatures (see section 2.2); however, further testing is required to fully understand the dynamics involved and to vet the material for use in applications as exotic as space launch vehicle upper stages.

Lastly, adsorbing large quantities of gas most likely has a negative effect on the ambient pressure thermal performance of the aerogel material (i.e. it would increase its thermal conductivity), which could cause issues during cryo-loading and ground hold portions of a launch countdown. Further investigation is necessary to determine the difference in effective thermal conductivity between "dry" and adsorbed aerogel blanket. The fear being that if the design value used is much lower than the actual it could lead to unacceptable levels of ice formation and LH_2 boiloff on the launch vehicle.

6. Future Work

Although this work presented testing that yielded some unexpected and intriguing results associated with a unique attribute of aerogel blanket insulation materials, there are numerous forward paths to pursue to advance the technology readiness level (TRL) with respect to LH_2 upper stage applications.

Use of the LN_2-argon combination for the test campaign was a necessary concession due to practical constraints such as lack of LH_2-based test equipment and lab safety; however, there are sufficient differences between it and the actual LH_2-air combination, that an effort should be conducted to understand the behavior of the material in more realistic test conditions. This will require a more elaborate LH_2-based calorimeter, but plans are underway to design and build such a device, deemed Cryostat-900 (C-900). C-900 will also be able to support investigations into cryo-pumping at LH_2 temperatures and characterize the thermal performance of potential insulation systems over the entire vacuum range, from high vacuum up 760 torr.

Significant effort is also necessary to devise potential aerogel-based insulation systems for upper stages and assess them for ascent survivability (thermal/wind loads, venting, etc.); manufacturability, processing, and physical application to the vehicle tank; and economic and mission architecture trade studies.

7. Conclusion

Aerogel blanket insulation material for application to LH_2 upper stage tanks was introduced, and the results of a complex test program examining a unique attribute of the material—vacuum induced, passive cooling—was presented. It was hypothesized that this cooling may be sufficient to reduce or eliminate the heat load on the LH_2 tank during ascent and early orbital operations of a mission, therefore the test setup aimed to recreate a situation similar to the cryo-loading/stabilization and ascent phases of a LH_2 upper stage launch. Due to various practical issues, LN_2 was used as a stand-in for LH_2, and argon was used in-place of air as the condensable background gas. The vertical-cylindrical cold-mass of the Cryostat-100 test instrument served as the upper stage tank and was wrapped with two layers of 10-mm Cryogel® aerogel blanket material and interspersed with numerous thermocouples. Single 0.127 mm aluminum foil sheets were also installed between, and on the outermost blankets layers to create a more "flight-forward" insulation system during one of the test sequences. The Cryostat-100 vacuum chamber contained the argon and was rapidly pumped-down to vacuum using three parallel vacuum pumps to simulate ascent.

Results of the testing revealed that the vacuum-induced release of argon from the aerogel blanket insulation layers provided enough cooling to the cold-mass tank to not only eliminate the incoming heat load, but further refrigerate the LN_2 below its boiling point, creating a backflow of ambient air into the LN_2 test chamber as a result. Thermocouple data showed blanket temperatures lower than the stainless-steel cold-mass during this backflow period, which is consistent with the reversed heat flow necessary to create a reversed test chamber flow rate. The lowest temperature recorded during ascent testing was 74 K—roughly 3 K below the boiling point of nitrogen, and 10 K below the freezing point of argon. Testing also uncovered potential issues related to pressure stabilization and "cryo-pumping" effects that require further examination.

A tremendous amount of additional investigation is necessary, and unique challenges overcome before aerogel-based insulation systems can be flight qualified for use on LH_2 upper stage tanks. However, the unexpected and intriguing results presented in this work suggest that such materials possess a potentially exploitable and powerful attribute in passive cooling, that just so happens to be available for the unique and specific application of LH_2-based space launch vehicle tanks. And if able to be harnessed, in conjunction with increased long duration in-space thermal performance afforded by the improved insulation system, could potentially unlock secondary upper stage missions and business cases that have traditionally been unrealizable due to high on-orbit boiloff rates.

8. References

[1] Kutter B. F., Cislunar-1000: Transportation supporting a self-sustaining Space Economy, AIAA SPACE 2016, Long Beach, CA, https://doi.org/10.2514/6.2016-5491

[2] Fesmire J. E. and Swanger A. M., Advanced cryogenic insulation systems, Proceedings of the 25th International Congress of Refrigeration, Montreal, Canada, (2019)

[3] Boer J., *The dynamical character of adsorption*, Oxford Clarendon Press (1966)

[4] Fesmire J. E., et. al., Cylindrical boiloff calorimeters for testing of thermal insulation systems, Advances in Cryogenic Engineering, IOP Conf. Series: Materials Science and Engineering **101**, (2015) 012056, doi:10.1088/1757 899X/101/1/012056

[5] Coffman B. E., et. al., AEROGEL BLANKET INSULATION MATERIALS FOR CRYOGENIC APPLICATIONS, Advances in Cryogenic Engineering, AIP Conference Proceedings **1218**, 913 (2010); https://doi.org/10.1063/1.3422458

[6] Fesmire J. E., Aerogel-Based Insulation Materials for Cryogenic Applications, IOP Conf. Series: Materials Science and Engineering 502, (2019) 012188 IOP Publishing doi:10.1088/1757-899X/502/1/012188

[7] Kutter B. F., et. al., Distributed Launch - Enabling Beyond LEO Missions, AIAA SPACE 2015, Pasadena, CA, https://doi.org/10.2514/6.2015-4593

[8] Fesmire J. E. and Johnson W. L., Cylindrical cryogenic calorimeter testing of six types of multilayer insulation systems, *Cryogenics*, Volume 89, (2018) pages 58-75, https://doi.org/10.1016/j.cryogenics.2017.11.004

[9] Fesmire J. E., Layered composite thermal insulation system for nonvacuum cryogenic applications, *Cryogenics*, Volume 74, (2016) pages 154-165, https://doi.org/10.1016/j.cryogenics.2015.10.008

[10] Dana, Leo I. "The Latent Heat of Vaporization of Liquid Oxygen-Nitrogen Mixtures." Proceedings of the American Academy of Arts and Sciences 60, no. 4 (1925): 241–67. https://doi.org/10.2307/25130052.